J. Chem. Sci. Vol. 123, No. 5, September 2011, pp. 733–741.

Computational study on decomposition kinetics of CH_3CFClO radical

HARI JI SINGH* and BHUPESH KUMAR MISHRA
Department of Chemistry, DDU Gorakhpur University, Gorakhpur, 273 009, India
e-mail: hjschem50@gmail.com

MS received 23 September 2009; revised 30 March 2011; accepted 13 June 2011

Abstract. The present study deals with the decomposition of haloalkoxy radical (CH_3CFClO) formed from 1,1-dichloro-1-fluoroethane (HCFC-141b) in the atmosphere. The study is performed using *ab-initio* quantum mechanical methods. Out of the three plausible pathways of decomposition of the titled species, the one that involved the C–C bond scission and the other occurring via Cl-atom elimination have been considered for detailed study. The geometries of the reactant, products and transition states involved in the decomposition pathways are optimized and characterized at MP2 level of theory using 6-311G(d,p) basis set. Single point energy calculations have been performed at G2(MP2) level of theory. The path involving the Cl-elimination is found to be dominant and found to occur with a barrier height of 3.6 kcal mol^{-1} whereas the C–C bond scission path proceeds with a barrier of 10.0 kcal mol^{-1}. The thermal rate constants for the above two decomposition pathways are evaluated using Canonical Transition State Theory (CTST) and these are found to be 2.9×10^8 s^{-1} and 4.3×10^5 s^{-1} for Cl-elimination and C–C bond scission respectively at 298 K and 1 atm. pressure. The existence of transition states on the corresponding potential energy surface is ascertained by the occurrence of only one imaginary frequency obtained during the frequency calculation. The Intrinsic Reaction Coordinate (IRC) calculation has also been performed to confirm the smooth connection of the TS to the reactant and the products.

Keywords. HCFC-141b; decomposition of HCFC; PES; canonical transition state theory.

1. Introduction

The deleterious effect of chlorofluorocarbons (CFCs) on the stratospheric ozone level is well documented.[1–3] The source of chlorine into the stratosphere includes the man made CFCs and naturally occurring processes. CFCs possess strong chemical stability and it is this characteristic that made them so attractive for a range of industrial applications. On the other hand, it is this property which makes CFCs environmental unfriendly. In particular, their strong resilience towards OH radical attack implies their unusual long lifetimes in the atmosphere.[4–6] Consequently, they reach the stratospheric region of the Earth's atmosphere in amounts virtually undiminished without being removed through any action. Once in the stratosphere they are broken down by UV light releasing chlorine atoms that initiate chain processes destroying ozone. In addition to their ability to destroy stratospheric ozone, the long atmospheric lifetime of the CFCs, makes these as potential 'greenhouse gases'.[5–7]

Global recognition of the adverse environmental impact of CFCs into the stratosphere led to an international effort to replace these compounds with environmentally acceptable alternatives. Serious efforts have been made during the recent past to search for its suitable replacements. Such efforts focused on hydrochlorofluorocarbons (HCFCs) and hydrofluorocarbons (HFCs). These compounds have been found to possess physico-chemical properties similar to that of CFCs and are widely accepted as alternatives to CFCs in industrial applications. The inclusion of at least one hydrogen atom in the CFCs makes it prone to attack by OH radicals leading to their breakdown in the troposphere where OH radicals are present in abundance. This leads to a significant reduction in the atmospheric lifetimes of HCFCs as compared to the CFCs providing a partial solution to protect the Earth atmosphere from the Greenhouse Effect. HCFCs have relatively short atmospheric lifetimes and lower ozone depletion potentials (ODPs) than CFCs. Its global warming potential is 0.09 over a 20-year time horizon relative to carbon dioxide.[8]

Based on the physical properties of HCFC-141b, this compound is regarded as the most suitable replace-

*For correspondence

ment for trichlorofluoromethane (CFC-11) and 1,1,2-trichloro-1,2,2-trifluoroethane (CFC-113), the most widely used CFCs in the industry as a foam blowing agent in polyurethane foam insulation and cleaning applications. HCFC-141b is mainly used as a blowing agent that is contained in closed-cell foam and is released to the atmosphere very slowly. In order to access the full impact of its potential use, knowledge of the detailed atmospheric chemistry of HCFC-141b is needed. Based on the AFEAS report[9] its global mean atmospheric concentration in Jan 1997 was estimated to be 5.7 ± 0.6 pptv (part per trillion by volume). As a blowing agent its use has increased significantly and its concentration in the atmosphere is significant to invite attention of scientists to study its fate in the atmosphere. Its tropospheric concentration[10,11] is large and has been estimated to be 0.46 ± 0.05 pptv as early as 1993. Because of its very low[5] ODP (0.088–0.11) some of HCFC-141b would be transported to the stratosphere. Its stratospheric concentration and life time[12] has been estimated to be 0.002 pptv and 68 ± 11 year respectively. Thus in the stratosphere, photolysis and reaction with O atom are important loss processes of such species. Wu and Carr[13] studied the photolysis of HCFC-141b by means of UV flash photolysis and time-resolved mass spectrometry. Photodissociation occurs primarily by scission of a C–Cl bond as given by reaction (1)

$$CH_3CFCl_2 + hv \longrightarrow CH_3CFCl + Cl. \quad (1)$$

The haloalkyl radical (CH_3CFCl) thus formed adds atmospheric molecular oxygen to give the peroxy radical ($CH_3CFClO_2\neg$) as follows

$$CH_3CFCl + O_2 \longrightarrow CH_3CFClO_2. \quad (2)$$

The rate constant for reaction (2) is determined to be 6.5×10^{-13} cm^3 $molecule^{-1}$ s^{-1} at 298 K and 1 atm pressure.[14] Peroxy radical formed via reaction (2) combines further with another peroxy radical in the atmosphere leading to the formation of the haloalkoxy radical CH_3CFClO as given by reaction (3).

$$CH_3CFClO_2 + CH_3CFClO_2 \longrightarrow CH_3CFClO + CH_3CFClO + O_2. \quad (3)$$

The kinetics of the recombination of peroxy radicals derived from HCFC-141b as given by reaction (3) has been studied by Wallington and Nielsen[15] using a pulse radiolysis technique and reported the rate constant to be 4.3×10^{-12} cm^3 $molecule^{-1}$ s^{-1}.

The chemistry of haloalkoxy radicals has been a subject of extensive experimental and theoretical investigations as these species are interesting intermediates in the atmospheric oxidation of halogenated hydrocarbons.[16–18] Due to the significant role played by haloalkoxy radicals formed from hydrochlorofluorocarbons in the destruction of a variety of organic compounds released into the atmosphere, studying the fate of CH_3CFClO formed from HCFC-141b is needed from the viewpoint of understanding its role in the atmospheric chemistry. To the best of our knowledge no theoretical study has been performed to elucidate the dissociative pathways of CH_3CFClO radical. Thus, there is a desirable need to perform high level *ab-initio* quantum mechanical calculations to determine the energetics involved during the decomposition of CH_3CFClO. The most plausible pathways for the decomposition of CH_3CFClO radicals are proposed to be C–C bond fission and Cl and H atoms elimination as given by reactions (4–6)

$$CH_3CFClO \longrightarrow CH_3 + C(O)FCl \quad (4)$$
$$\longrightarrow CH_3C(O)F + Cl \quad (5)$$
$$\longrightarrow H + CH_2C(O)FCl. \quad (6)$$

In the present investigation, we performed a computational study on the decomposition pathways of CH_3CFClO radical involving C–C bond scission and Cl and H atoms elimination as given by reactions (4–6) using high-level molecular orbital methods. Rate constants for the above channels considered have been calculated by utilizing Canonical Transition State Theory (CTST). Attempts have been made to search for transition states on the corresponding potential energy surfaces and energy barriers are calculated. Intrinsic Reaction Coordinate (IRC) calculations have also been performed to ascertain the smooth transition from reactants to products via transition state.

2. Computational method

All *ab-initio* molecular orbital calculations[19] performed during the course of the present investigation were carried out using the GAUSSIAN 03 series of program.[20] The geometries of reactant, products and transition states had been fully optimized at UMP2(full)/6-311G(d,p)[21,22] level of theory. Vibrational frequencies were calculated at the same level to characterize the stationary points. The stable minima are characterized by the existence of positive vibrational frequencies. The transition state has been characterized by the occurrence of only one imaginary frequency. Intrinsic Reaction Coordinate (IRC)[23] were also performed at

UMP2(full)/6-311G(d,p) to ascertain that each transition state was linked to the desired reactants and products and the transition was smooth. The zero-point energies (ZPE) of various species were also calculated utilizing the same level of theory at which optimization was made. Energy values were refined by performing single point energy calculations at QCISD(T)/6-311G(d,p) and MP2/6-311+G(3df,2p) levels at the optimized geometries. Based on these values, G2(MP2)[24] energies were calculated. The G2(MP2) method is a modified version of G2 using MP2 instead of MP4 for the basis set extension corrections and is considered to reasonably approximate the full G2 method at a substantially reduced computational cost. The G2(MP2) energy is calculated as:[24]

$$\mathrm{E\,[G2\,(MP2)]} = \mathrm{E_{base}} + \Delta\mathrm{E\,(MP2)} + \mathrm{HLC} + \mathrm{ZPE},$$

where

$$\mathrm{E_{base}} = \mathrm{E}\left[\mathrm{QCISD\,(T)\,/6\text{-}311G\,(d,p)}\right],$$

$$\begin{aligned}\Delta\mathrm{E\,(MP2)} \;=\; & \mathrm{E}\left[\mathrm{MP2/6\text{-}311{+}G\,(3df,2p)}\right] \\ & -\mathrm{E}\left[\mathrm{MP2/6\text{-}311G\,(d,p)}\right], \text{and}\end{aligned}$$

HLC and ZPE are the High Level Correction and Zero Point Energy respectively. An empirical equation[24,25] for HLC is added to account for any remaining deficiencies in the energy calculations. It is based on the number of α and β electrons and can be determined as:

$$\mathrm{HLC} = -0.00481\mathrm{n}_\beta - 0.00019\mathrm{n}_\alpha,$$

where n_α and n_β are the number of α and β valence electrons with $\mathrm{n}_\alpha \geq \mathrm{n}_\beta$.

3. Results and discussion

The fate of haloalkoxy radical (CH_3CFClO) is envisaged to occur via Rxs (4–6). The detailed calculation performed during the present investigation revealed that the endothermicity of reaction (6) was more than 38 kcal mol^{-1} which would make it less probable as compared to reactions (4) and (5) whose reaction enthalpies have been found to be −4.29 and −19.85 kcal mol^{-1} respectively as listed in table 1. This is also supported by the free energy change data included in table 1. Results show that free energy change for H atom elimination during the decomposition of CH_3CFClO (Rx6) occurs with +31.55 kcal mol^{-1} which would make it improbable to proceed in the forward direction. Thus, the plausible fate of CH_3CFClO in the atmosphere has been considered to be its thermal decomposition occurring via Rxs (4) and (5). The two dominant decomposition pathways considered via reactions 4 and 5 involve transition states TS1 and TS2 respectively. Optimized geometries of reactant, products and transition states obtained at UMP2(full)/6-311G(d,p) level of theory are shown in figure 1 and corresponding geometrical parameters are given in table 2. In order to see the influence of basis set on the geometrical parameters of the species concerned, calculations have been performed with double diffuse basis set such as 6-311++G(d,p). The results are also included in table 2 showing that the extended basis set has very little effect on the geometry of the titled species involved during the present calculation. Results obtained during frequency calculations for reactant, products and transition states at UMP2(full)/6-311G(d,p) level are given in table 3. Results show that the reactant and products have stable minima on their potential energy surface and these are characterized by the occurrence of all real vibrational frequencies. Results given in table 3 also show the occurrence of only one imaginary frequency at 691 and 857 cm^{-1} for TS1 and TS2 respectively. These frequencies are analysed using GaussView[26] visualization program. Visualization of the imaginary frequency gives a qualitative confirmation of the existence of transition states connecting reactant and products. Intrinsic reaction path calculations (IRC)[23] have also been performed for each transition state. The IRC plots for

Table 1. Thermochemical data for the decomposition channels of CH_3CFClO calculated at UMP2(full)/6-311G(d,p) level of theory.

Reaction channels	${}_r\Delta H^\circ$ (298 K) (kcal.mol^{-1})	${}_r\Delta G^\circ$ (298 K) (kcal.mol^{-1})	ΔS° (298 K) (cal.mol^{-1} K^{-1})
$CH_3CFClO \longrightarrow CH_3 + C(O)FCl$	−4.29	−15.54	37.73
$CH_3CFClO \longrightarrow CH_3C(O)F + Cl$	−19.85	−28.79	30.0
$CH_3CFClO \longrightarrow H + CH_2C(O)FCl$	38.29	31.55	22.60

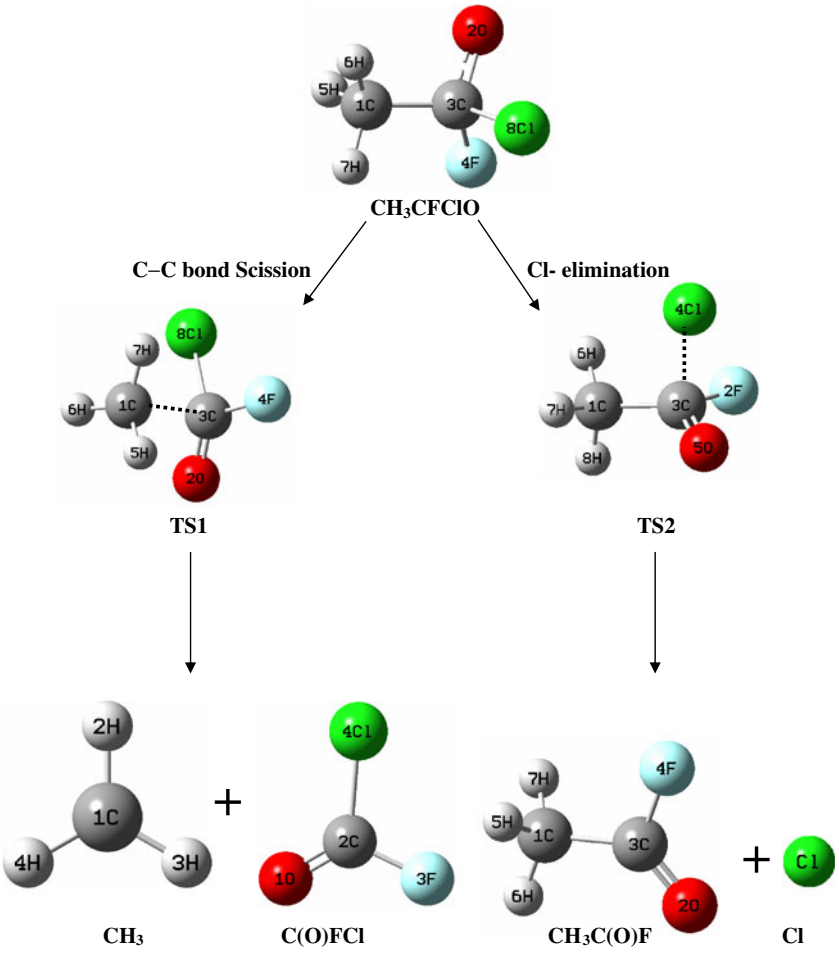

Figure 1. Optimized geometries of reactant, products and transition states involved in the decomposition of CH_3CFClO using UMP2(full)/6-311G(d,p) method.

TS1 and TS2 shown in figure 2 reveal that the transition state structure connects smoothly the reactant and the product sides. The energies of reactant, transition states and products obtained in the IRC calculations are given in table 4 and they are in good agreement with the individually optimized values at UMP2(full)/6-311G(d,p) level of theory. Visualization of the optimized structure of TS1 further reveals the elongation of C–C bond length from 1.516 Å to 1.909 Å (36%) at MP2 level. At the same time a shrinkage of the C–O distance from 1.337 Å to 1.189 Å (11%) and forming a carbon–oxygen double bond has also been observed. These results are in accordance with that obtained in an earlier study performed at the same level by Hou *et al.*[27] for C–C bond scission in a similar haloalkoxy radical, CH_3CHClO in which they found an increase of C–C bond distance from 1.524 to 2.000 Å (31%) together with a decrease in the C–O bond distance from 1.354 to 1.198 Å (11%) in the transition state structure. The analysis of TS2 obtained during the present study for the Cl-elimination reveals the elongation of C–Cl bond length from 1.789 Å to 2.040 Å (14%) at MP2 level. Hou *et al.*[27] also reported an increase of 18% in C–Cl bond distance in CH_3CHClO. The results obtained during the present study further reveals a simultaneous shrinkage of C–O bond distance from 1.337 Å to 1.247 Å in TS2 also as given in table 2.

The total energies of the reactant (CH_3CFClO), products ($CH_3C(O)FCl$, $CH_3C(O)F$, and F and transition states (TS1 and TS2) calculated using MP2 and QCISD(T) methods at UMP2(full)/6-311G(d,p) optimized geometries. Zero-point energy of the species concerned are obtained at MP2/6-311G(d,p) level and corrected with a scale factor of 0.96 to partly eliminate the known systematic errors.[28] Zero-point corrected total energies using different basis sets are given in table 5 for species and the transition state involved in the decomposition via C–C bond scission whereas the same is given in table 6 for Cl-elimination. Energy values at a higher level using G2(MP2) method are

Table 2. Structural parameters of reactant, products and transition states involved in CH_3CFClO decomposition at UMP2(full)/6-311G(d,p) level (first line) and UMP2(full)/6-311++G(d,p) (second line).

	CH_3CFClO	TS1	TS2	CH_3	C(O)FCl	CH_3 C(O)F
Bond length (Å)						
R (C1-C3)	1.516	1.909	1.500	–	–	1.495
	1.515	1.907	1.500	–	–	1.494
R (C3-O2)	1.337	1.189	–	–	–	1.187
	1.339	1.190	–	–	–	1.188
R (C3-O5)	–	–	1.247	–	–	–
	–	–	1.244	–	–	–
R (C2-O1)	–	–	–	–	1.178	–
	–	–	–	–	1.180	–
R (C1-H4)	–	–	–	1.078	–	–
	–	–	–	1.078	–	–
R (C1-H5)	1.091	1.083	–	–	–	1.091
	1.091	1.083	–	–	–	1.091
R (C1-H6)	1.088	1.082	1.087	–	–	1.087
	1.088	1.082	1.088	–	–	1.087
R (C1-H7)	1.089	1.084	1.091	–	–	1.091
	1.090	1.084	1.087	–	–	1.091
R (C3-F4)	1.367	1.357	–	–	–	1.360
	1.374	1.364	–	–	–	1.366
R (C3-Cl4)	–	–	2.040	–	–	–
	–	–	2.039	–	–	–
R (C3-Cl8)	1.789	1.797	–	–	–	–
	1.783	1.789	–	–	–	–
R (C3-F2)	–	–	1.342	–	–	–
	–	–	1.350	–	–	–
R (C2-F3)	–	–	–	–	1.328	–
	–	–	–	–	1.333	–
R (C2-Cl4)	–	–	–	–	1.731	–
	–	–	–	–	1.723	–
Bond angle (deg)						
A (C3-C1-H5)	108.7	100.7	–	–	–	109.1
	108.8	100.6	–	–	–	109.2
A (C3-C1-H6)	110.0	103.0	110.3	–	–	109.9
	109.9	102.8	110.3	–	–	109.8
A (C3-C1-H7)	107.9	99.3	109.5	–	–	109.1
	107.9	99.2	109.5	–	–	109.2
A (C1-C3-F4)	109.1	98.0	–	–	–	109.9
	109.0	98.0	–	–	–	109.9
A (C1-C3-Cl8)	111.7	99.9	–	–	–	–
	112.1	100.0	–	–	–	–
A (C1-C3-O2)	109.3	100.2	–	–	–	129.3
	109.8	100.5	–	–	–	129.7
A (C1-C3-O5)	–	–	123.1	–	–	–
	–	–	123.6	–	–	–
A (C1-C3-Cl4)	–	–	106.2	–	–	–
	–	–	106.6	–	–	–
A (H2-C1-H3)	–	–	–	120.0	–	–
	–	–	–	120.0	–	–
A (O1-C2- F3)	–	–	–	–	124.3	–
	–	–	–	–	123.9	–
A (O1-C2-Cl4)	–	–	–	–	126.2	–
	–	–	–	–	126.5	–

Table 3. Unscaled vibrational frequencies of reactant, products and transition states in CH_3CFClO decomposition at UMP2(full)/6-311G(d,p) level of theory.

Species	Vibrational frequencies (cm^{-1})
CH_3CFClO	234, 263, 301, 417, 438, 534, 687, 910, 952, 1103, 1179, 1252, 1417, 1491, 1500, 3114, 3215, 3237
TS1	**691i**, 220, 249, 285, 414, 456, 570, 697, 763, 788, 1015, 1156, 1446, 1463, 1740, 3147, 3823, 3335
TS2	**857i**, 242, 261, 294, 410, 426, 587, 833, 992, 1046, 1248, 1406, 1435, 1489, 1502, 3112, 3211, 3248
$CH_3C(O)F$	144, 419, 577, 608, 855, 1024, 1080, 1228, 1423, 1489, 1498, 1921, 3112, 3199, 3238
CH_3	421, 1446, 1446, 3181, 3374, 3374
C(O)FCl	421, 511, 679, 775, 1118, 1924

also listed in tables 5 and 6. Energy barriers for C–C bond scission and Cl-elimination channels occurring via TS1 and TS2 respectively are also given in table 7. These values are evaluated from the zero-point energy corrected total energies of tables 5 and 6. Literature survey reveals that there are no experimental or theoretical data available for the comparison of these energy barriers for the corresponding decomposition pathways of CH_3CFClO radical. In order to ascertain the reliability of the calculated values, we tried to compare our results with the values calculated by Hou *et al.*[27] for a similar compound CH_3CHClO using G2(MP2,SVP)//UMP2(full)/6-31G(d) which yielded the energy barrier for C–C bond scission to be 12.2 kcal mol^{-1}. The corresponding value obtained in CH_3CFClO during the present investigation using G2(MP2)//UMP2(full)/6-311G(d,p) method is found to be 10.0 kcal mol^{-1}. A detailed analysis of the optimized structures of these two radicals at the same level of calculation shows that the replacement of H atom by a more electronegative F atom results in an increase of C–C bond from 1.509 to 1.516 A. Increase of C–C bond distance in the case of CH_3CFClO would reflect the weakening of the C–C bond in CH_3CFClO as compared to CH_3CHClO radical. This in turn may be responsible for the lowering in the energy barrier for its decomposition. Thus, the calculated energy barrier of 10.0 kcal mol^{-1} for the C–C bond scission in CH_3CFClO obtained during the present study at G2(MP2)//UMP2(full)/6-311G(d,p) would be relied upon. This gives us a confidence that energy barrier calculated using G2(MP2) method on the geometries optimized at UMP2(full)/6-311G(d,p) yields reliable values for the decomposition channels considered in the present study. An energy diagram constructed with the zero-point corrected energies data relative to the ground state energy of CH_3CFClO arbitrarily taken as zero is plotted in figure 3. The barrier height of 3.6 kcal mol^{-1} for Cl-elimination is much lower than that of the C–C bond scission. This makes the Cl-elimination pathway as the dominant process for the dissociation of this haloalkoxy radical in the atmosphere which is in accordance with the experimental observations made by Bhatnagar and Carr[29] for a similar haloalkoxy radical CF_3CFClO. Spin contamination is the artificial mixing of different electronic spin-states. This can occur when an approximate orbital-based wave function is represented in an unrestricted form and can affect the geometry and spin density. The expectation value of the total spin-squared operator $<S^2>$ is a measure of the spin contamination. Spin contamination is not important for the CH_3CFClO radical because $<S^2>$ is in the range of 0.758 to 0.76 at UMP2(full)/6-311G(d,p) before annihilation. These values are only slightly higher than the expected value of $<S^2> = 0.75$ for doublets.

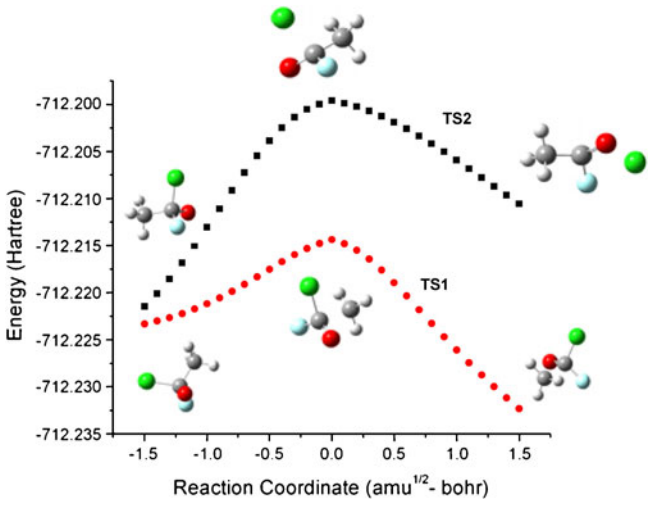

Figure 2. IRC plots for the transition states TS1 (C–C bond scission) and TS2 (Cl-elimination) for thermal decomposition of CH_3CFClO.

3.1 *Rate constants*

The rate constants of reactions (4) and (5) of CH_3CFClO radical decomposition are calculated using

Table 4. Energies of reactant, transition states and products obtained in IRC calculations performed at UMP2(full)/6-311G(d,p) geometries.(unit:hartree).

Species	IRC	UMP2(full)/6-311G(d,p)
TS1	−712.199	−712.199
Reactant (CH_3CFClO)	−712.221	−712.225
Products (CH_3 + C(O)FCl)	−712.210	−712.226
TS2	−712.214	−712.214
Reactant (CH_3CFClO)	−712.223	−712.225
Products (CH_3CFO + Cl)	−712.232	−712.257

Table 5. Zero-point energy corrected total energies for species involved in C–C bond scission from CH_3CFClO decomposition. Geometries were optimized at UMP2(full)/6-311G(d,p) level.(unit: hartree).

Method	CH_3CFClO	TS1	CH_3	C(O)FCl
MP2/6-311G(d,p)	−712.051834	−712.029256	−39.678271	−672.383155
MP2/6-311+G(3df,2p)	−712.261115	−712.241867	−39.702399	−672.732988
QCISD(T)/6-311G(d,p)	−712.119888	−712.097851	−39.703276	−672.417006
G2(MP2)	−712.398666	−712.382633	−39.717422	−672.854462
ZPE UMP2/6-311G(d,p)	0.050693	0.048019	0.030172	0.012377

Canonical Transition State Theory (CTST)[30] that involves a semi-classical one-dimensional multiplicative tunneling correction factor as given by the following expression:

$$k = \Gamma\,(T)\,\frac{k_B T}{h}\,\frac{Q^{\ddagger}_{TS}}{Q_R}\,exp\frac{-\Delta E}{RT}, \qquad (7)$$

where Γ(T) is the tunnelling correction factor at temperature T. $Q^{\ddagger}_{TS}$ and Q_R are the total partition functions for the transition state and reactant respectively. ΔE, k_B and h are the barrier height including ZPE, Boltzmann's and Planck's constants respectively. One can adopt the simple and computationally inexpensive Wigner's method[31] for the estimation of the tunnelling correction factor using the expression

$$\Gamma\,(T) = 1 + \frac{1}{24}\left(\frac{h\nu^{\ddagger}}{k_B T}\right)^2, \qquad (8)$$

where $\nu^{\#}$ is the imaginary frequency at the saddle point. However, the tunnelling correction factor, Γ(T) should be negligible for heavier atom/group as in the reactions studied. The partition functions for the respective transition state and reactant at 298 K are obtained from the harmonic vibrational frequencies calculated at the UMP2/6-311G(d,p) level and computed with the zero of energy being the first vibrational level. The rate constants for decomposition channels involving C–C bonds scission and Cl-elimination in CH_3CFClO decomposition are calculated to be $k_{C-C} = 4.3 \times 10^5\ s^{-1}$ and $k_{C-Cl} = 2.9 \times 10^8\ s^{-1}$ respectively at 298 K and 1 atm pressure. We could not find any experimental data available in the literature to make a comparison with the calculated values obtained during the present investigation. Therefore, we performed kinetic calculations for a similar haloalkoxy radical, CH_2FCHFO for which experimental rate constant is available. Our calculation reveals a rate constant of $111 \times 10^4\ s^{-1}$ for C–C bond

Table 6. Zero-point energy corrected total energies for species involved in Cl- elimination from CH_3CFClO decomposition. Geometries were optimized at UMP2(full)/6-311G (d,p) level. (unit: hartree).

Method	CH_3CFClO	TS2	$CH_3C(O)F$	Cl
MP2/6-311G(d,p)	−712.051834	−712.042391	−252.500319	−459.585137
MP2/6-311+G(3df,2p)	−712.261115	−712.253112	−252.654187	−459.630301
QCIST (T)/6-311G(d,p)	−712.119888	−712.111525	−252.542397	−459.603285
G2(MP2)	−712.398666	−712.392885	−252.726551	−459.688639
ZPE UMP2/6-311G(d,p)	0.050693	0.049551	0.049714	0.000

Table 7. Calculated energy barriers in kcal mol^{-1}.

Method	C–C bond scission	Cl-elimination
MP2/6-311G(d,p)	14.2	5.9
MP2/6-311+G(3df,2p)	12.0	5.0
QCISD (T)/6-311G(d,p)	13.8	4.9
G2(MP2)	10.0	3.6

scission whereas the detailed calculation performed by Hou *et al.*[32] resulted it to be 200 × 10^4 s^{-1}. The experimental value for the same reaction has been reported to be 6 × 10^4 s^{-1} in the lower limit by Wallington *et al.*[33]

However, based on an analogy with the decomposition of other oxy-radicals for C–C bond scission, our calculated value comes out to be of the same order of magnitude.[34] The A-factor is evaluated from the expression

$$A = \frac{k_B T}{h} \frac{Q^{\ddagger}_{TS}}{Q_R}, \tag{9}$$

where the terms have their usual meaning. The calculated value of the A-factor for reaction occurring via C–C bond scission is found to be 0.8 × 10^{13} s^{-1} which is also in good agreement with the value of 1.1 × 10^{13} s^{-1} reported by Caralp *et al.*[35] for CH_3CH_2O. Similarly, the rate constant for Cl-elimination pathways is calculated to be 2.9 × 10^8 s^{-1} with the associated A-factor of 6.5 × 10^{13} s^{-1}. No theoretical and experimental data are available for Cl-elimination reaction channel for a haloethoxy radical and the present investigation may give a base for future experimental studies.

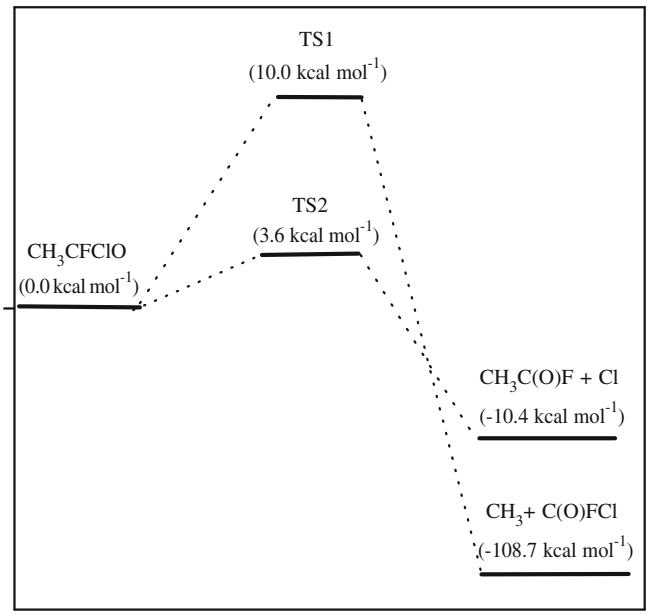

Figure 3. Relative energy diagram for the thermal decomposition of CH_3CFClO at G2(MP2) level.

4. Conclusion

The stationary point on the potential energy surface for the thermal decomposition of CH_3CFClO radical is investigated using *ab-initio* quantum mechanical method. The geometry optimization of reactant, products and transition states are carried out at UMP2(full)/6-311G(d,p) level of theory. The energetics of decomposition pathways of CH_3CFClO radical has been examined. The results show that the most dominant decomposition pathways for CH_3CFClO is the Cl-elimination occurring via C–Cl bond scission involving a barrier height of 3.6 kcal mol^{-1} as compared to the other channel occurring via C–C bond breaking which utilizes 10.0 kcal mol^{-1}. The rate constants for Cl-elimination and C–C bond scission are found to be 2.9 × 10^8 and 4.3 × 10^5 s^{-1} at 298 K and 1 atm. pressure respectively.

Acknowledgements

One of the authors, BKM is thankful to University Grants Commission (UGC), New Delhi for providing fellowship under its Special Assistance Program (SAP) sanctioned to the Department of Chemistry, Deen Dayal Upadhyay (DDU) University, Gorakhpur. The financial support from Council of Scientific and Industrial Research (CSIR), New Delhi is also acknowledged. This work is also sponsored by UP State Government under its Center of Excellence Program to this University.

References

1. Solomon S 1990 *Nature* **347** 6291
2. Molina M J and Rowland F S 1974 *Nature* **249** 810
3. Rowland F S and Molina M J 1994 *Chem. Eng. News.* **8** 72
4. Weubbles D J 1983 *J. Geophys. Res.* **88** 1433
5. *Scientific assessment of stratospheric ozone*, 1989, Vol II AFEAS Report, World Meteorological Organization, Global Ozone Research and Monitoring Project, Report No-20
6. Wayne R P 2001 *The chemistry of atmospheres* (Oxford: Clarendon Press)
7. Ravishankara A R and Lovejoy E R 1994 *J. Chem. Soc. Faraday Trans.* **90** 2159
8. Jonathan S N and Stephanle R S 1992 *Environ. Sci. Tech.* **26** 739

9. AFEAS (Alternative Fluorocarbons Environmental Acceptability Study) 1997 *Production, Sales and Atmospheric Release of Fluorocarbons through 1995* (Washington, DC: AFEAS Program Office)
10. Shirai T and Makide Y 1998 *Chem. Lett.* **4** 357
11. Oram D E, Reeves C E, Penkett S A and Fraser P J 1995 *Geophys. Res. Lett.* **22** 2741
12. Lee J M, Sturges W T, Penkett S A, Oram D E, Schmidt U, Engel A and Bauer R 1995 *Geophys. Res. Lett.* **22** 1369
13. Wu Fuxiang and Carr R W 1995 *J. Phys. Chem.* **99** 3128
14. DeMore W B, Sander S P, Howard C J, Ravishankara A R, Golden D M, Kolb C E, Hampson R F, Molina M J and Kurylo M J 1992 *Chemical kinetics and photochemical data for use in stratospheric modeling*, Evaluation Number 10, JPL Publication 92–20
15. Wallington T J and Nielsen O J 1991 *Int. J. Chem. Kinet.* **23** 785
16. Brasseur G P and Orlando J J (ed) 1999 *Atmospheric chemistry and global change* (New York: Oxford University Press)
17. Wallington T J, Hurley M D, Francheboud J M, Orlando J J, Tyndall G S, Sehested J, Møgelberg T E and Nielsen O J 1996 *J. Phys. Chem.* **100** 18116
18. Zellner R (ed) 1999 *Global aspect of atmospheric chemistry* (Darmstadt: SteinKopff)
19. Hehre W J, Radom L, Schleyer P V R and Pople J A 1986 *Ab initio Molecular orbital theory* (New York: Wiley)
20. Frisch M J et al 2004 *Gaussian 03 (Revision C.02)* (Wallingford CT: Gaussian Inc)
21. Moller C and Plesset M S 1934 *Phys. Rev.* **46** 618
22. Hariharan P C and Pople J A 1973 *Theo. Chem. Act.* **28** 213
23. Gonzalez C and Schlegel H B 1990 *J. Phys. Chem.* **94** 5523
24. Curtiss L A, Raghavachari K and Pople J A 1993 *J. Chem. Phys.* **98** 1293
25. Curtiss L A, Redfern P C, Smith B J and Radom Leo 1996 *J. Chem. Phys.* **104** 5148
26. Frisch A, Nielsen A B and Holder A J 2003 *GaussView Users Manual* (Gaussian Inc, PA, USA)
27. Hou H, Wang B and Gu Y 2000 *J. Phys. Chem. A* **104** 1570
28. Scott A P and Radom L 1996 *J. Phys. Chem.* **100** 16502
29. Bhatnagar A and Carr R W 1995 *J. Phys. Chem.* **99** 17573
30. Truhlar D G, Garrett B C and Klippenstein S J 1996 *J. Phys. Chem.* **100** 12771
31. Wigner E P 1977 *Z. Phys. Chem.* **81** 2572
32. Hou H, Wang B and Gu Y 2000 *Phys. Chem. Chem. Phys.* **2** 61
33. Wallington T J, Hurley M D, Ball J C, Ellermann T, Nielsen O J and Sehested J 1994 *J. Phys. Chem.* **98** 5435
34. Stevens J E, Khayat R A J, Radkevich O and Brown J 2004 *J. Phys. Chem.* **108** 11354
35. Caralp F, Devolder P, Fittschen C, Gomez N, Hippler H, Mereau R, Rayez M T, Striebel F and Viskolcz B 1999 *Phys. Chem. Chem. Phys.* **1** 2935